

# Alzheimer Precursor Protein Interaction with the Nogo-66 Receptor Reduces Amyloid- $\beta$ Plaque Deposition

James H. Park,<sup>1</sup> David A. Gimbel,<sup>1</sup> Tadzia GrandPre,<sup>1</sup> Jung-Kil Lee,<sup>1</sup> Ji-Eun Kim,<sup>1</sup> Weiwei Li,<sup>2</sup> Daniel H. S. Lee,<sup>2</sup> and Stephen M. Strittmatter<sup>1</sup>

<sup>1</sup>Department of Neurology, Yale University School of Medicine, New Haven, Connecticut 06510, and <sup>2</sup>BiogenIdec Inc., Cambridge, Massachusetts 02140

Pathophysiologic hypotheses for Alzheimer's disease (AD) are centered on the role of the amyloid plaque  $A\beta$  peptide and the mechanism of its derivation from the amyloid precursor protein (APP). As part of the disease process, an aberrant axonal sprouting response is known to occur near  $A\beta$  deposits. A Nogo to Nogo-66 receptor (NgR) pathway contributes to determining the ability of adult CNS axons to extend after traumatic injuries. Here, we consider the potential role of NgR mechanisms in AD. Both Nogo and NgR are mislocalized in AD brain samples. APP physically associates with the NgR. Overexpression of NgR decreases  $A\beta$  production in neuroblastoma culture, and targeted disruption of NgR expression increases transgenic mouse brain  $A\beta$  levels,  $A\beta$  plaque deposition, and dystrophic neurites. Infusion of a soluble NgR fragment reduces  $A\beta$  levels, amyloid plaque deposits, and dystrophic neurites in a mouse transgenic AD model. Changes in NgR level produce parallel changes in secreted APP $\alpha$  and  $A\beta$ , implicating NgR as a blocker of secretase processing of APP. The NgR provides a novel site for modifying the course of AD and highlights the role of axonal dysfunction in the disease.

**Key words:** Alzheimer's disease;  $\beta$ -amyloid plaque; Nogo; transgenic mice; Nogo-66 receptor; gene targeting; amyloid precursor protein; APP

## Introduction

Amyloid plaques and neurofibrillary tangles are the principal pathologic hallmarks that accompany neuronal loss in the dementia of Alzheimer's disease (AD) (Hardy and Selkoe, 2002; Selkoe and Schenk, 2003). The amyloid  $A\beta$  peptide is derived proteolytically from amyloid precursor protein (APP) and is the major constituent of the amyloid plaque in AD. Although the rate of  $A\beta$  peptide release from APP is implicated in AD pathophysiology, there is less certainty regarding which forms of  $A\beta$  result in neuronal dysfunction and by what mechanism this occurs. The transformation of monomeric  $A\beta$  to large amyloid plaque deposits proceeds through several intermediate steps, and intermediate forms may be causative in the neuronal dysfunction of AD (Klein, 2002; Walsh et al., 2002b).  $A\beta$  peptides have been shown to interact with several macromolecules that might potentially contribute to pathology. Such  $A\beta$ -binding proteins include, but are not limited to, the receptor for advanced glycation end products (Yang et al., 1996), the low-affinity NGF receptor p75-NTR (Kuner et al., 1998) and nicotinic acetylcholine receptors (Wang et al., 2000; Dineley et al., 2001; Nagele et al., 2002). The cellular effects of  $A\beta$  application have included cell death, altered synap-

tic transmission, stimulation of neurite outgrowth, and inhibition of neurite outgrowth (Walsh et al., 2002a; Kamenetz et al., 2003). It remains unclear which cellular effects depend on specific molecular interactions and are most relevant to the ability of  $A\beta$  to cause dementia.

There are several observations that connect APP and  $A\beta$  to axonal mechanisms. Many amyloid plaques, the so-called "neuritic plaques," exhibit a cluster of dystrophic neurites surrounding their edge (Lombardo et al., 2003). This suggests that aberrant, ineffective sprouting mechanisms are activated in the vicinity of  $A\beta$  deposits. Recent data have demonstrated that local  $A\beta$  deposits are dependent on axonal input, implying that the principal source of  $A\beta$  is peptide released from the presynaptic ending of the axon (Lazarov et al., 2002; Sheng et al., 2002). In brain trauma, APP accumulation in transected axons is one of the better markers of injured axons (Otsuka et al., 1991; Scott et al., 1991; Gentleman et al., 1993). Furthermore, APP has been implicated as an adaptor protein for kinesin I-based axonal transport (Kamal et al., 2001). Most recently, intriguing studies have demonstrated physical interactions between Reticulon family proteins (including Nogo) and BACE1 ( $\beta$ -secretase activity of the  $\beta$ -site APP-cleaving enzyme), one of the proteases responsible for  $A\beta$  production from APP (He et al., 2004). For these reasons, we considered the potential connection between those molecular processes that regulate axonal sprouting in the adult CNS and the APP/ $A\beta$  pathologic process. One pathway implicated in adult axonal CNS sprouting is the Nogo/Nogo receptor (NgR) pathway (Chen et al., 2000; GrandPre et al., 2000, 2002; Prinjha et al., 2000; Fournier et al., 2001; Kim et al., 2003, 2004; Li and Strittmatter, 2003; McGee and Strittmatter, 2003; Lee et al., 2004; Li et al.,

Received June 9, 2005; revised Dec. 4, 2005; accepted Dec. 15, 2005.

This work was supported in part by grants from the National Institutes of Health, the McKnight Foundation, and the Institute for the Study of Aging (S.M.S.) and by an Institutional Medical Scientist Training grant (J.H.P.). S.M.S. is a member of the Kavli Institute of Neuroscience at Yale University. We thank the Harvard Brain Tissue Resource Center for human brain tissue samples and S. S. Sisodia for helpful discussions, N2A-APPsw cells, and anti-C-terminal APP antibody 369.

Correspondence should be addressed to Stephen M. Strittmatter, Department of Neurology, Yale University School of Medicine, P.O. Box 208018, New Haven, CT 06510. E-mail: stephen.strittmatter@yale.edu.

DOI:10.1523/JNEUROSCI.3291-05.2006

Copyright © 2006 Society for Neuroscience 0270-6474/06/261386-10\$15.00/0

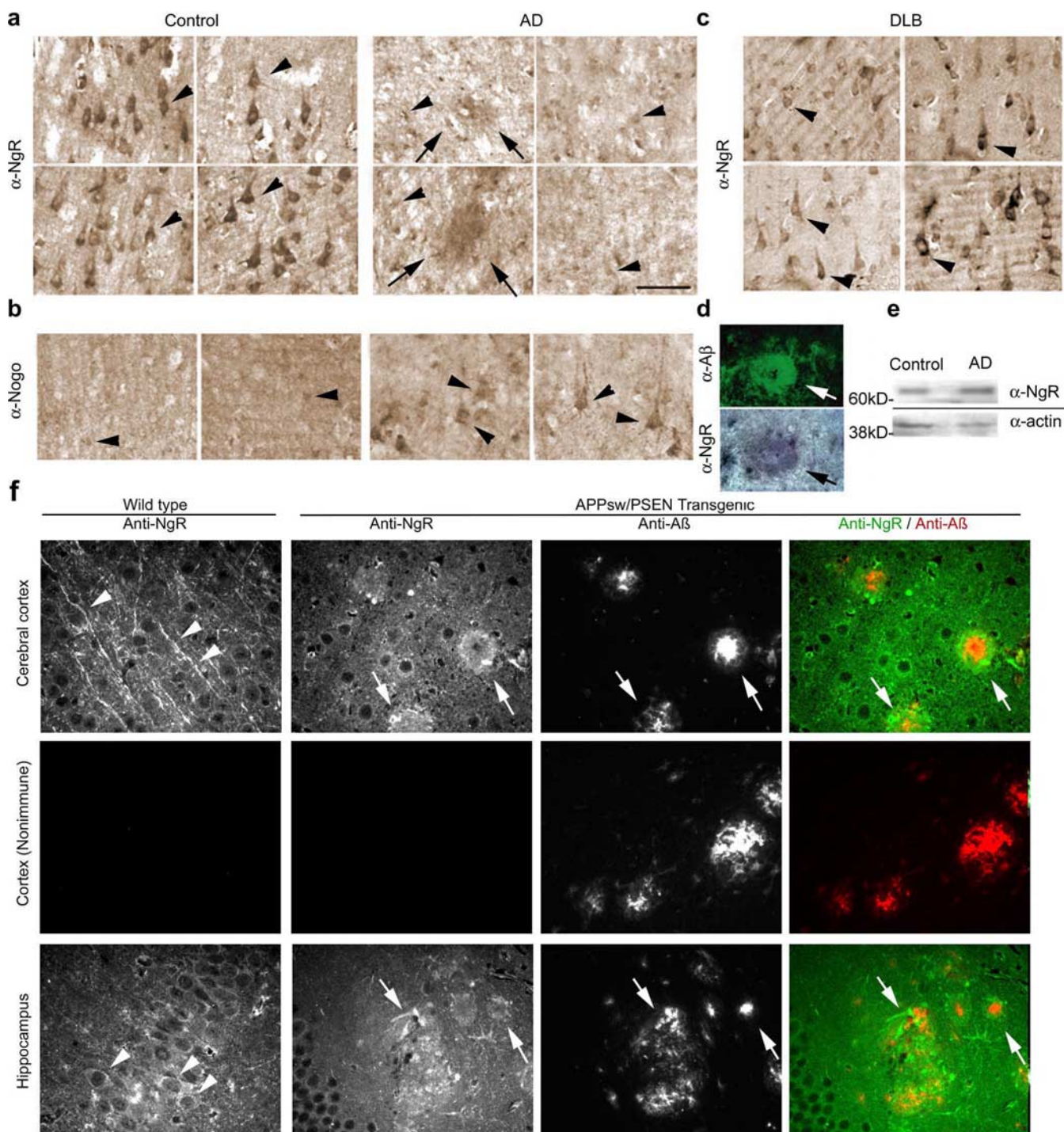


**Figure 1.** Altered Nogo and NgR localization in human AD brain. **a–c**, Human brain samples from age-matched control samples, AD, or diffuse Lewy body dementia (DLB) were processed for anti-NgR or anti-Nogo-A immunohistochemistry as indicated. All samples are from the hippocampus. Note the reduced cellular NgR localization in AD and the enhanced cellular Nogo localization in the AD samples (arrowheads, cellular staining). Some amyloid plaques are NgR immunoreactive (arrows). **d**, The colocalization of NgR and A $\beta$  in plaques is shown in higher magnification at the bottom right (arrows). **e**, Anti-NgR immunoblot demonstrates the specificity of the anti-NgR antibody and the unchanged NgR level in the AD brain compared with controls. Two additional control and two additional AD cases had staining patterns similar to that shown here. Anti-actin immunoblot demonstrates similar protein loading. **f**, Sections of cerebral cortex or hippocampus from wild-type or APPsw/PSEN transgenic mice of 9 months age were stained with anti-NgR or nonimmune IgG (green in merged image) and anti-A $\beta$  antibody (6E10, red in merged image). Brains were fixed in paraformaldehyde, sectioned in paraffin, and treated with formic acid before staining. In wild-type brain, axonal profiles are detected in the cerebral cortex, and cell soma are stained in the hippocampus (arrowheads). In transgenic brain, cellular and axonal staining is reduced, but periplaque NgR immunoreactivity (arrows) is detected.

2004). We find that NgR interacts with APP and A $\beta$  to limit A $\beta$  accumulation *in vivo*.

## Materials and Methods

Human brain tissue samples were obtained from the National Institutes of Health-supported Harvard Brain Tissue Resource Center with no per-

sonal identifying information. Anti-Nogo-A and anti-NgR rabbit antibodies and immunohistological methods have been described previously (Wang et al., 2002), as have NgR expression vectors, alkaline phosphatase (AP)-Nogo-66 protein, and the purified soluble function-blocking NgR ectodomain [NgR(310)ecto-Fc] (GrandPre et al., 2000; Fournier et al., 2001, 2002; Lee et al., 2004; Li et al., 2004). The anti-NgR antibody raised



in goat was from R & D Systems (Minneapolis, MN) (AF1440). The AP-A $\beta$  and AP-APP proteins were produced by the same method as AP-Nogo-66. The binding of AP fusion proteins to transfected COS-7 cells has been described previously (GrandPre et al., 2000; Fournier et al., 2001, 2002; Li et al., 2004). N2A neuroblastoma cells stably expressing the Swedish form of APP (APP<sup>Swe</sup>) and the 369 anti-C-terminal-APP antibody were generous gifts from S. S. Sisodia (University of Chicago, Chicago, IL) (Thinakaran et al., 1996). The anti-N-terminal-APP 5228 antibody, the anti-A $\beta$ <sub>1–17</sub> 6E10 antibody, and the anti-C-terminal-APP 5352 antibody were obtained from Chemicon (Temecula, CA). The anti-A $\beta$  4G8 antibody and the anti-C-terminal-APP 51–2700 antibodies were from Signet Laboratories (Dedham, MA) and Zymed Laboratories (South San Francisco, CA), respectively. The anti-secreted APP (sAPP) $\beta$ -specific 6A1 antibody was from Immunobiological Laboratories (Gunma, Japan). A $\beta$ <sub>1–40</sub> and A $\beta$ <sub>40–1</sub> with an N-terminal biotin tag were synthesized at the W. M. Keck Biotechnology facility at Yale University.

For covalent cross-linking studies, adult rat brain was homogenized in PBS plus protease inhibitor mixture (Roche Products, Welwyn Garden City, UK). The particulate fraction was collected by centrifugation at 100,000  $\times$  g for 20 min. Membranes were resuspended in PBS (1 ml/gm brain wet weight) and incubated with 3 mM bis(sulfosuccinimidyl) suberate (BS<sup>3</sup>) for 1 h at 4°C. Unreacted cross-linker was quenched by addition of Tris-HCl, pH 7.6, to 0.1 M. Particulate material was again collected by centrifugation, and then membrane protein was solubilized with 1% Triton X-100. The detergent extract was subjected to nonimmune IgG or anti-NgR (1D9) immunoprecipitation using protein A/G Sepharose (Pierce, Rockford, IL) and analyzed by anti-NgR plus anti-APP immunoblot.

The generation of NgR<sup>−/−</sup> mice has been described previously (Kim et al., 2004). In this line, exon II containing the entire mature coding region is deleted and no NgR protein is produced. In the studies here, the NgR mutant allele from a 129/sv embryonic stem cell was backcrossed to C57BL/6J for four to six generations before breeding with APP<sup>Swe</sup>/presenilin-1 (PSEN-1)( $\Delta$ E9) transgenic mice. In all experiments, littermate mice carrying one APP<sup>Swe</sup>/PSEN-1( $\Delta$ E9) transgene and either heterozygous or homozygous for the NgR null mutation were compared with one another. Transgenic APP<sup>Swe</sup>/PSEN-1( $\Delta$ E9) (Borchelt et al., 1997; Jankowsky et al., 2003) mice were from The Jackson Laboratory (Bar Harbor, ME) (stock #04462) and were obtained on a mixed strain background as described by the provider.

A $\beta$  ELISA assays were performed according to the instructions of the manufacturer (Biosource, Camarillo, CA). A $\beta$  plaques in parasagittal sections of 4% paraformaldehyde-fixed brain were detected immunohistologically with anti-A $\beta$ <sub>1–17</sub> 6E10 antibody after 0.1 M formic acid treatment for antigen recovery. Plaque area was quantitated using NIH Image as a percentage of total cerebral cortical area for three sections from each animal. Neuritic dystrophy was visualized by staining with monoclonal anti-synaptophysin antibodies (Sigma, St. Louis, MO) in parasagittal paraffin-embedded sections. The area of cerebral cortex and hippocampus occupied by clusters of dystrophic neurites was measured as a percentage of total area, using the outer border of increased staining by the same method as for A $\beta$  plaque load. For analysis of sAPP $\alpha$  and A $\beta$  levels from brain extracts, forebrain was extracted with 0.1 M formic acid, neutralized with Tris, and clarified by centrifugation at 10,000  $\times$  g.

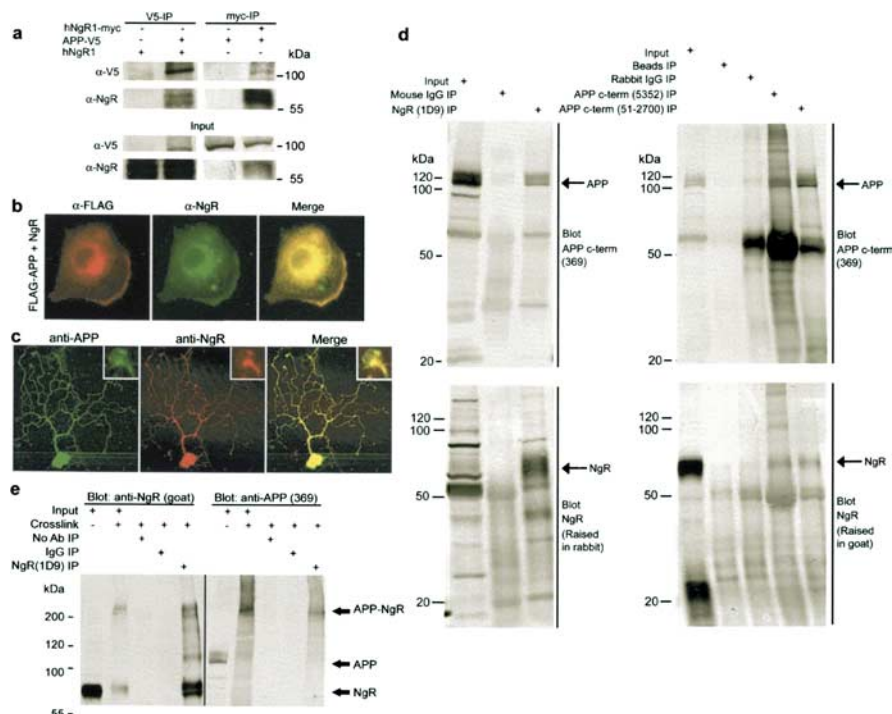


**Figure 2.** Physical interaction of NgR and APP. *a*, Epitope-tagged version of human APP and NgR were expressed in HEK-293T cells alone or in combination. Immunoprecipitates of APP show detectable NgR, and immunoprecipitates of NgR exhibit APP immunoreactivity. Twelve percent of the input protein is loaded in the bottom panels. *b*, Transfected COS-7 cells expressing FLAG-APP (red) and NgR (green) were examined by double-labeled immunohistochemistry. *c*, APP and NgR localization in neurons. Mouse postnatal day 5 DRG neurons were stained with anti-APP (green) and anti-NgR antibodies (red). The insets show higher magnification of one growth cone. *d*, Rat brain homogenates were immunoprecipitated with 1D9 (monoclonal anti-NgR), control IgG, 5352 (anti-C-terminal-APP), and 51–2700 (anti-C-terminal-APP). Coimmunoprecipitation of APP and NgR was detected by immunoblotting with the indicated antibodies. Seven percent of the input protein is loaded in the indicated lanes. *e*, Particulate fractions of adult rat brain were treated for 1 h at 4°C with 3 mM BS<sup>3</sup>. Detergent solubilized protein was immunoprecipitated with anti-NgR antibody as in *d*. The immunoprecipitates were examined for NgR and APP immunoreactivity. Note the formation of a high-molecular-weight complex that is immunoreactive for both NgR and APP.

To administer NgR(310)ecto-Fc protein to mice, animals were anesthetized with isoflurane and oxygen, and a burr hole was drilled in the skull. A cannula (Alzet brain infusion kit II; Alza, Palo Alto, CA) was introduced into the right lateral ventricle at stereotaxic coordinates 0.6 mm posterior and 1.2 mm lateral to bregma and 2.0 mm deep to the pial surface. The cannula was held in place with cyanoacrylate, and the catheter was attached to a subcutaneous osmotic minipump (Alzet 2004; Alza). The pump delivered 0.25  $\mu$ l/h for 28 d of a 1.2 mg/ml solution of NgR(310)ecto-Fc or rat IgG in PBS. Pumps were replaced after 28 d and connected to the same cannula.

## Results

### Altered NgR and Nogo subcellular localization in AD

As a first direct step toward considering a role for the Nogo-NgR system in AD, human brain sections from AD cases and controls were examined histologically for Nogo-A and NgR localization (Fig. 1*a,b,d*). Tissue from the hippocampus and Brodmann's area 20/36 were examined in six control and six AD cases. In the control adult human brain, Nogo-A immunoreactivity is detectable in a diffuse granular pattern in the neuropil of these brain regions with little cellular staining. Here, we have focused on gray matter in which a majority of Nogo is neuronal, not oligodendrocytic in origin, as in white matter (Wang et al., 2002). In all of the AD cases, there is a dramatic shift of Nogo-A immunoreactivity to cell bodies (Fig. 1*b*, arrowheads). NgR localization in the AD brain is shifted in the opposite manner (Fig. 1*a*). In control cases, the highest concentration of the NgR protein is found in cell soma (arrowheads). Both the pattern of staining in human sam-

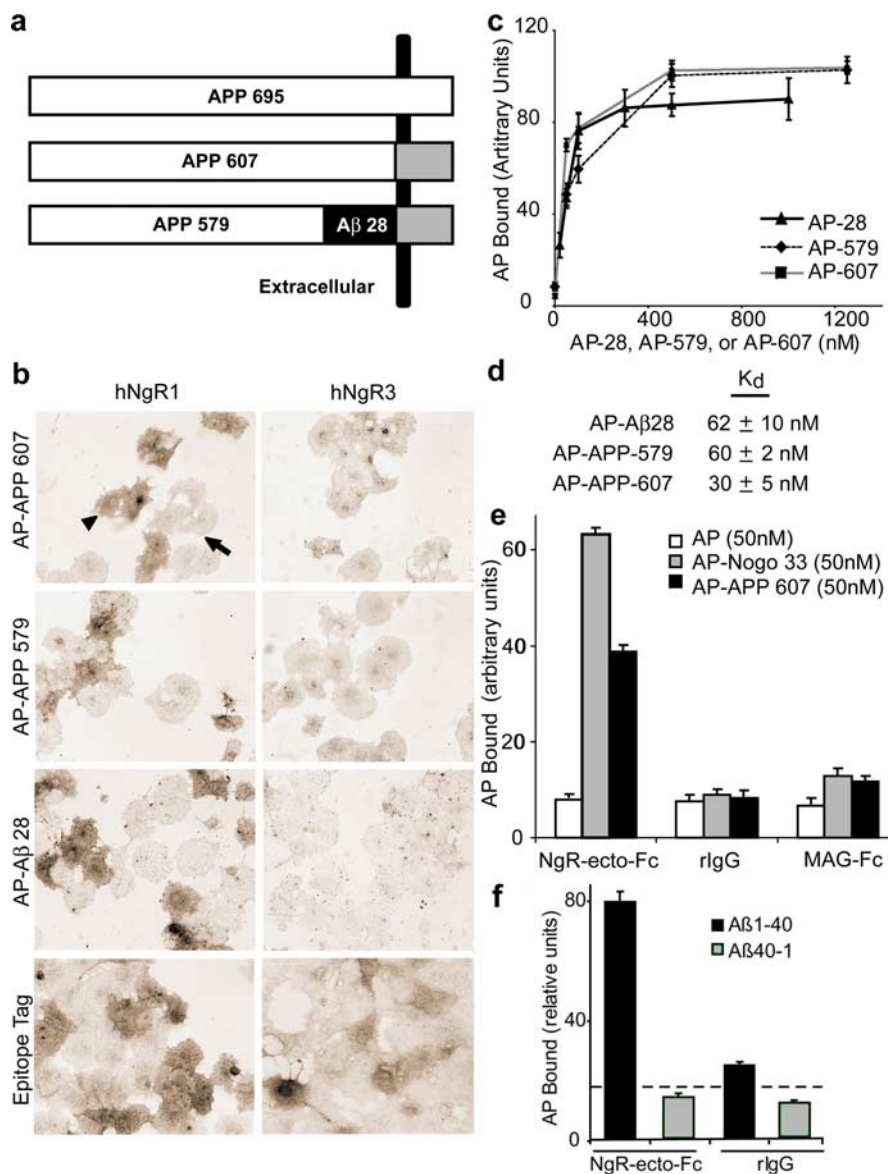


**Figure 3.** APP ectodomain binds to NgR1-expressing cells. **a**, A schematic illustrates the cellular orientation of APP and the fragments that were used to express AP fusion proteins. **b**, COS-7 cells were cultured with transfection of human NgR1 or human NgR3 expression plasmid, and their respective expressions were verified by epitope-tag immunohistochemistry. Fifty nanomolar solutions of AP-APP607, AP-APP579, and A $\beta$ <sub>28</sub>-AP were allowed to bind to transfected cells for 2 h before washing, fixation, heat inactivation of endogenous AP, and enzymatic detection of bound fusion protein. Note the dark reaction product by arrowhead derived in cultures expressing NgR1 but not NgR3. An untransfected cell is labeled by the arrow. This is one of five experiments with similar results. **c**, **d**, Binding of AP-A $\beta$ <sub>28</sub>, APP579, and APP607 to NgR1-expressing COS-7 cells from an experiment as in **a** was measured as a function of ligand concentration from 5 to 1250 nM. Data are means  $\pm$  SEM from one of three experiments with similar results. The calculated K<sub>d</sub> is noted in **d**. **e**, Purified NgR-ecto(310)-Fc, MAG-Fc, or BSA (100 ng of each protein) was coated onto microtiter wells. After blockade of nonspecific sites with excess BSA, the wells were exposed to 50 nM AP, AP-Nogo 33, or AP-APP607. Data are the means  $\pm$  SEM from three similar experiments. Note the selective binding of either Nogo(1–33) or APP607 to NgR-coated wells. **f**, The binding of 100 nM biotin-A $\beta$ <sub>1–40</sub> or biotin-A $\beta$ <sub>40–1</sub> to immobilized NgR(344)-ecto-Fc or IgG (100 ng of each protein) was detected by retention of streptavidin-AP.

ples and the previous murine studies suggest that the cellular NgR immunoreactivity is neuronal (Wang et al., 2002). Four AD brain samples exhibit little cellular NgR staining but diffuse immunoreactivity in the neuropil and in plaque-like deposits. Neither NgR nor Nogo-A colocalizes with neurofibrillary tangles or dystrophic neurites recognized by an antibody directed against hyperphosphorylated Tau protein (data not shown). Specificity of staining was demonstrated by antigen blockade and by the recognition of a single immunoreactive protein on immunoblots of

human samples (Fig. 1*e* and data not shown). By immunoblot analysis, the total level of NgR is not altered in AD samples (Fig. 1*e*). The absence of NgR staining in cell bodies is not attributable to a complete absence of neurons, as can be appreciated clearly in the adjacent sections stained with Nogo-A antibodies (Fig. 1, compare *a*, *b*). Altered NgR localization is not observed in a different dementing illness, diffuse Lewy body dementia (Fig. 1*c*). In addition to the shift of NgR out of the cell soma, the protein is concentrated in amyloid plaques (Fig. 1*a*, *d*, arrows). Double immunohistochemistry for A $\beta$  and NgR demonstrates their colocalization in these deposits (Fig. 1*d*). These findings suggest that the Nogo/NgR pathway might have either a primary or secondary role in AD pathology.

We also examined NgR localization in a transgenic mouse model of AD, the APP<sup>swe</sup>/PSEN-1( $\Delta$ E9) double-transgenic mice (Borchelt et al., 1997; Jankowsky et al., 2003). NgR-immunoreactive processes are prominent in the cerebral cortex (Fig. 1*f*, arrowheads, top left), whereas neuronal cell bodies are stained in the CA3 region of the hippocampus of wild-type mice (Fig. 1*f*, arrowheads, bottom left). NgR staining of cell bodies is less prominent in the transgenic mice (arrowheads), and axons are not readily apparent in the APP<sup>swe</sup>/PSEN-1( $\Delta$ E9) cerebral cortex. A fraction of the protein is detected at the border of amyloid plaques (Fig. 1*f*, arrows). NgR staining is most prominent at the circumference of intense A $\beta$  deposits (Fig. 1*f*, merged image). The transgenic mouse model confirms the existence of altered NgR localization in AD.

### APP interacts with NgR in transfected cells and brain

Based on these observations of Nogo and NgR localization, we considered whether there might be direct interactions between these proteins and APP. Epitope-tagged versions of the proteins were expressed in human embryonic kidney HEK-293T cells and immunoprecipitation studies were performed. APP specifically associates with NgR (Fig. 2*a*) but not with Nogo-A in these studies (data not shown). If APP and

NgR are to associate in living cells, then at least a portion of the proteins must colocalize at the subcellular level. Both proteins are known to be associated with lipid rafts (Fournier et al., 2002; Eehalt et al., 2003), and double-immunohistochemical studies reveal a nearly complete overlap of the distribution for two proteins in transfected cells and primary neurons (Fig. 2*b*, *c*). The physical association of endogenous NgR and APP was also examined in rat brain homogenates. Immunoprecipitates of APP contain NgR immunoreactivity, and anti-NgR isolates possess APP



protein detected with different APP antibodies (Fig. 2*d*). To verify that the physical association of NgR with APP occurs within intact tissue and is not dependent on detergent solubilization, covalent cross-linking studies of rat brain membranes were performed (Fig. 2*e*). Approximately half of NgR is covalently coupled by BS<sup>3</sup> treatment into a high-molecular-weight complex with an apparent molecular weight ( $M_r$ ) of 200–250 kDa. The high  $M_r$  NgR-immunoprecipitable complex is also strongly immunoreactive for APP. The apparent molecular mass of this complex is greater than would be predicted for a 1:1 NgR/APP complex and may reflect aberrantly slow migration of a cross-linked complex or the presence of a more complicated structure including two copies of NgR or additional protein species. We conclude that a fraction of APP and NgR are physically associated within neurons.

We sought to determine which region of APP might interact with NgR. Because NgR is a glycosylphosphatidylinositol (GPI)-anchored protein, any direct interaction must be mediated by the APP extracellular (ecto) domain. We created fusion proteins containing various portions of the APP ectodomain fused to AP. At nanomolar concentrations, the ecto-APP-AP protein binds to NgR-expressing COS cells but not to vector-transfected COS cells or to COS cells expressing the related protein NgR3 (Fig. 3). The APP extracellular domain is cleaved by  $\beta$ -secretase enzyme into two fragments. As AP fusion proteins, the sAPP $\beta$  fragment (APP597) and  $\beta$ <sub>1–28</sub> ectodomain fragment both exhibit affinity for NgR (Fig. 3*b–d*). Thus, the physical interaction of APP with NgR occurs through both amino and carboxyl segments of the ectodomain of APP. Furthermore, both  $\beta$ -secretase substrates (APP607) and  $\beta$ -secretase products (APP597 and  $\beta$ <sub>1–28</sub>) can interact with NgR.

The association of APP and NgR might be direct or indirect. To distinguish these possibilities, we immobilized purified NgR protein and examined the binding of APP-AP ligand in the absence of other cellular constituents (Fig. 3*e*). The APP ligand clearly binds to NgR under these minimal conditions, demonstrating a direct association of the two proteins.

The AP fusion method required a truncated  $\beta$ <sub>1–28</sub> fragment to maintain protein ligand solubility. We used synthetic forms of  $\beta$ <sub>1–40</sub> to verify that the endogenous peptide also interacts with NgR. In the ELISA format, the interaction of biotin- $\beta$ <sub>1–40</sub> with NgR is easily measured above background (Fig. 3*f*). In contrast, the reverse  $\beta$ <sub>40–1</sub> peptide does not interact with immobilized NgR.  $\beta$ <sub>1–40</sub> binding to cell surface NgR was examined using biotinylated peptide, fluorescent avidin, and cell sorting (Fig. 4). The binding of  $\beta$ <sub>1–40</sub> to COS-7 cells is dramatically enhanced by NgR expression, and this binding is suppressed by anti-NgR an-

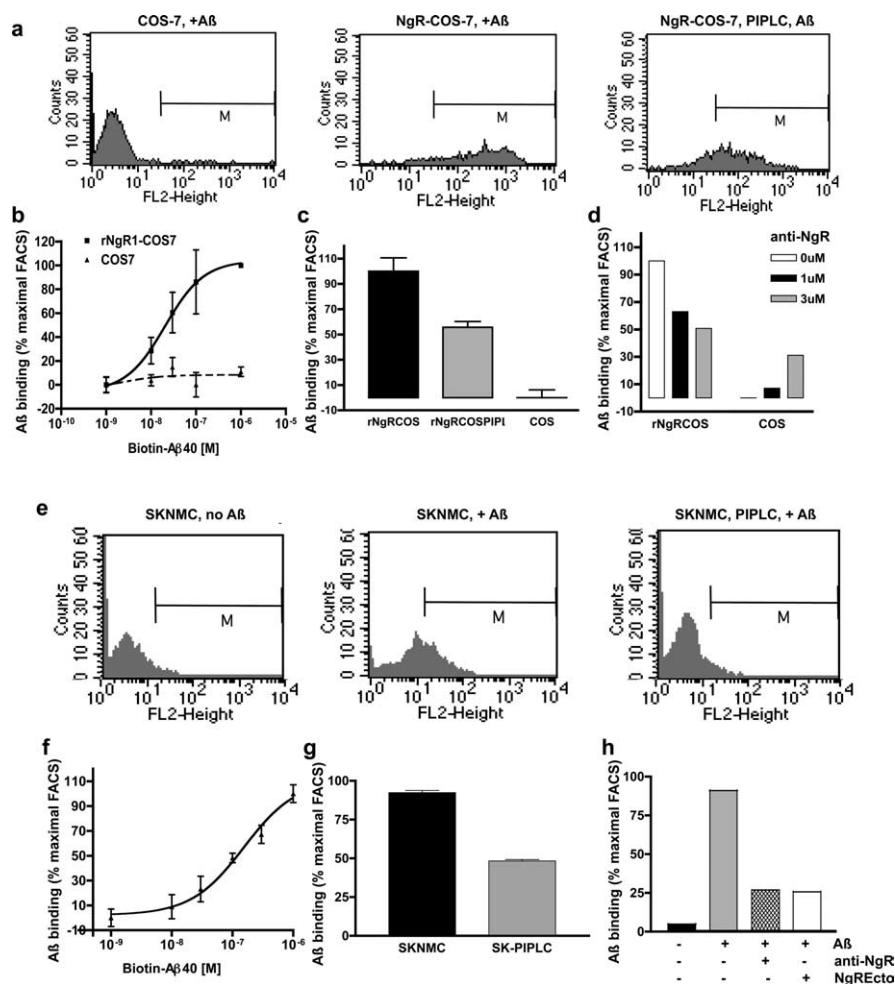


**Figure 4.**  $\beta$ <sub>1–40</sub> binds to NgR-expressing cells. *a–d*, Binding of 100 nM biotinylated  $\beta$ <sub>1–40</sub> to COS-7 cells transfected with vector or rat NgR expression plasmid. Bound  $\beta$  was detected by fluorescence-activated cell sorting (FACS) after incubation with Alexa488-conjugated streptavidin (*a*). Some cells were treated with 1 U of PI-PLC for 1 h at 37°C to release GPI-anchored proteins from the cell surface immediately before binding (*a*, *c*). The gating criterion for the quantitation of binding is illustrated by a bar, M. The dose dependence for binding was assessed with the indicated concentrations of  $\beta$  (*b*). The NgR1 antibody 7E11 was added before biotinylated 100 nM  $\beta$  to displace binding from NgR-expressing COS-7 cells (*d*). *e–h*, The fluorescence-activated cell sorting method was used to detect biotin- $\beta$ <sub>1–40</sub> binding to human neuroblastoma SK-NMC cells (*e*).  $\beta$ <sub>1–40</sub> bound dose dependently (*f*) and the binding was diminished after PI-PLC treatment (*e*, *g*). *h*, Biotinylated  $\beta$ <sub>1–40</sub> was displaced from SK-NMC by anti-NgR antibodies (2E10, 1  $\mu$ M) and by soluble NgR(344)ecto-Fc (1  $\mu$ M). Data are means  $\pm$  SEM from three to six experiments with similar results.

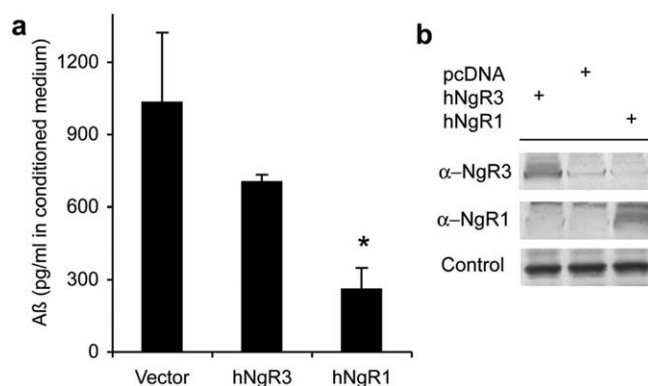


**Figure 5.** NgR expression decreases  $\beta$  formation by neuroblastoma cells. Neuroblastoma N2A cells stably expressing APP<sub>swe</sub> (Thinakaran et al., 1996) were transiently transfected with control plasmid or vectors directing the expression of hNgR3 or hNgR1. *a*,  $\beta$ <sub>1–40</sub> ELISA was performed on conditioned medium. \* $p$   $\leq$  0.025; the decrease in A $\beta$  is significant and represents data from four independent transfections. *b*, N2A cell lysate was examined by immunoblot with the indicated antibodies to verify expression.

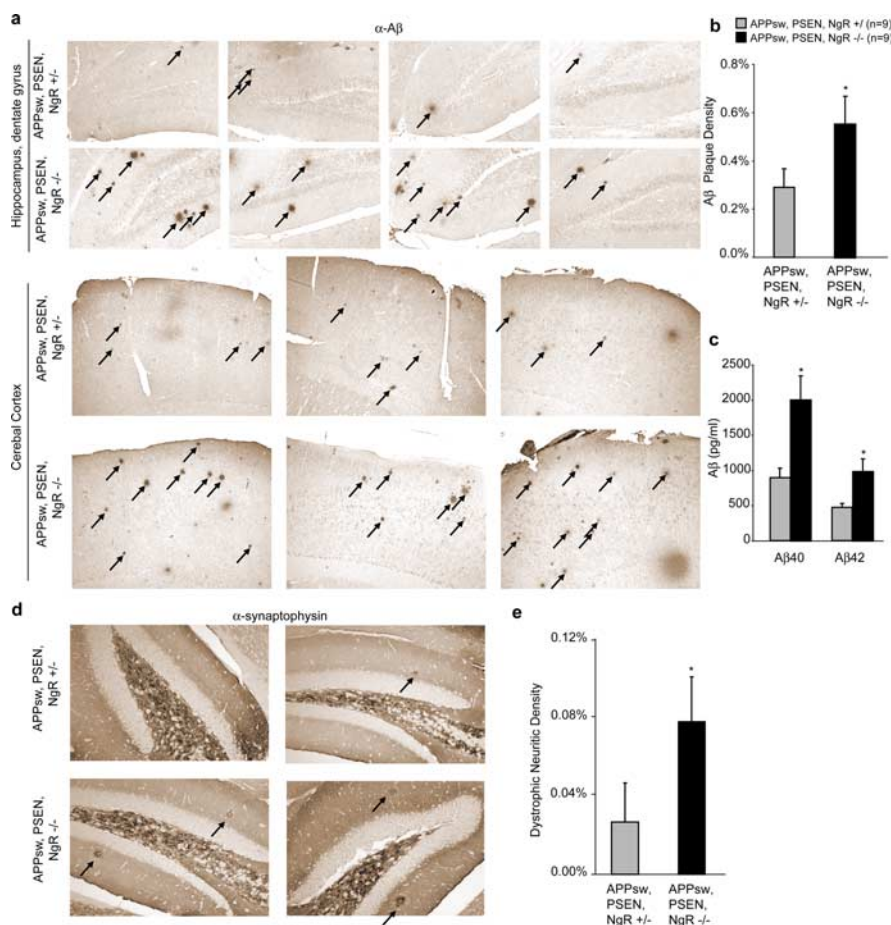


**Figure 6.** Enhanced A $\beta$  and neuritic dystrophy in FAD transgenic mice lacking NgR. Mice coexpressing human APPsw/PSEN-1( $\Delta$ E9) and heterozygous for a null allele of NgR were intercrossed with  $NgR^{-/-}$  mice. At 6 months of age, littermate-matched mice expressing APPsw/PSEN-1( $\Delta$ E9) and either  $NgR^{+/+}$  or  $NgR^{-/-}$  were killed. Brain tissue was analyzed by immunohistochemistry and ELISA. **a, b**, Arrows indicate examples of plaque deposits in hippocampal dentate gyrus and cerebral cortex. Plaque densities were quantified from nine mice in each group and are significantly different ( $*p \leq 0.05$ , Student's *t* test). **c**, A $\beta_{1-40}$  and A $\beta_{1-42}$  levels were assessed by ELISA and are significantly different ( $*p \leq 0.04$  level, Student's *t* test) for nine mice of each genotype. **d, e**, Anti-synaptophysin-immunoreactive dystrophic neurites are illustrated (arrows, **d**). The percentage of area occupied by synaptophysin-positive dystrophic neurites is reported in **e**. Data are means  $\pm$  SEM from nine mice per group.  $*p < 0.05$ , Student's *t* test; the decrease in dystrophic neurites is significant.

tibody or by phosphatidylinositol-specific phospholipase C (PI-PLC) treatment to cleave the GPI-anchored NgR protein from the cells. The binding of A $\beta$  to SKNMC neuroblastoma cells containing endogenous NgR is also suppressed by anti-NgR antibodies, PI-PLC treatment, and soluble NgR-ectodomain decoy receptor. Thus, NgR provides a high-affinity binding site for APP and A $\beta$ .

#### NgR overexpression reduces A $\beta$ production in neuroblastoma cells

One of the critical steps in AD is the proteolytic production of A $\beta$  from APP. The effect of NgR on this processing was assessed in N2A neuroblastoma cells stably expressing APPsw (Fig. 5*a, b*). Conditioned medium from these cells contains a significant level of A $\beta$  (Thinakaran et al., 1996). Expression of endogenous NgR in the N2A cell line is low and undetectable by immunoblots. Overexpression of NgR, but not NgR3, in the APPsw-N2A cells significantly suppresses A $\beta$  production. NgR may limit the access of processing secretases to their APP substrate by either direct steric hindrance or an indirect mechanism.

#### Increased A $\beta$ accumulation in mice lacking NgR

To examine the significance of the NgR/APP interaction on APP processing *in vivo*, the APPsw/PSEN-1( $\Delta$ E9) double-transgenic mouse (Borchelt et al., 1997; Jankowsky et al., 2003) was bred onto a NgR null background (Fig. 6). Brain sections and tissue extracts were examined for A $\beta$  at 6 months of age. Compared with littermate-matched control mice, the absence of NgR significantly increases the accumulation of both A $\beta$  plaque and immunoreactive A $\beta$  (Fig. 6*a–c*). The similar elevations in A $\beta_{1-40}$  and A $\beta_{1-42}$  suggest that  $\gamma$ -secretase site preference is not altered by the absence of NgR.

One consequence of A $\beta$  deposition is the formation of dystrophic neurites in and around plaques. To determine whether NgR absence might alter dystrophic neurite formation separately from A $\beta$  accumulation, serial sections of the hippocampal dentate gyrus were examined for anti-synaptophysin immunoreactivity (Fig. 6*d, e*). The twofold increased A $\beta$  plaque density of the  $NgR^{-/-}$  animals is mirrored by a comparable increase in neuritic dystrophy. Thus, NgR modulates neuritic dystrophy in parallel with A $\beta$  levels. We conclude that endogenous NgR has a role in restricting brain A $\beta$  accumulation.

#### NgR(310)ecto-Fc treatment reduces A $\beta$ plaque deposition

To increase NgR/APP interactions *in vivo*, soluble NgR(310)ecto-Fc protein was infused into APPsw/PSEN-1( $\Delta$ E9) double-transgenic mice (Borchelt et al., 1997; Jankowsky et al., 2003). The NgR(310)ecto-Fc protein contains the entire leucine-rich repeat ligand-binding domain of the NgR fused to the Fc portion of IgG (Lee et al., 2004; Li et al., 2004). To assess the specificity of action of this protein in brain, we examined the distribution of binding sites for NgR(310)ecto-Fc in wild-type and APPsw/PSEN-1( $\Delta$ E9) double-transgenic mouse brain by virtue of the rat Fc moiety (Fig. 7). The NgR(310)ecto-Fc protein, but not control IgG, associates with myelinated fiber tracts and prominently labels the corpus callosum and intraparenchymal fiber tracts in wild-type brain (Fig. 7*a*). This is consistent with binding to the previously described myelin ligands of NgR. In transgenic brain, the protein also labels A $\beta$ -positive plaques (Fig. 7*b*). Whereas control IgG itself exhibits some detectable nonspecific binding for dense A $\beta$  plaques, NgR(310)ecto-Fc binding is also detectable at the border of plaques in which lower levels of A $\beta$  are found (Fig. 7*c*).

NgR(310)ecto-Fc was administered intracerebroventricularly by continuous infusion from 6- to 8-month-old mice with an Alzet minipump (Alza). Control APPsw/PSEN-1( $\Delta$ E9) mice received rat IgG because both the NgR and the Fc moiety were of rat origin. The total dose of protein infused was 0.4 mg/mouse over 56 d, corresponding to 0.29 mg/kg body weight per day. After



56 d, mice were killed, and the distribution of NgR(310)ecto-Fc and rat IgG was assessed (Fig. 8). The pattern of *in vivo* binding after intracerebroventricular infusion matches that for NgR(310)ecto-Fc binding to tissue sections. Myelinated tracts are labeled in white matter and in gray matter throughout the forebrain, demonstrating that the infused protein has access to the parenchyma of the brain. Some infused IgG is trapped in dense A $\beta$  plaques, but specific NgR(310)ecto-Fc binding to the plaque periphery exceeds the nonspecific trapping of control protein.

For these treated mice, brain A $\beta$  levels were measured by ELISA, and A $\beta$  deposition into amyloid plaques was assessed by anti-A $\beta$  immunohistochemistry. In the NgR(310)ecto-Fc mice, the deposition of immunoreactive A $\beta$  into plaque is significantly reduced (Fig. 9*a,b*). The total level of both A $\beta_{1-40}$  and A $\beta_{1-42}$  decreases by 50% in the brain (Fig. 9*c*). The ratio of A $\beta_{40}$  to A $\beta_{42}$  is not altered in the treated group, arguing that  $\gamma$ -secretase function was not significantly modulated by soluble NgR. There is a tight correlation between A $\beta$  levels and amyloid plaque deposition, suggesting that NgR(310)ecto-Fc alters APP/A $\beta$  metabolism to a greater extent than A $\beta$  aggregation itself (Fig. 9*d*).

Because dystrophic neurite formation occurs in and around amyloid plaques and NgR can regulate neurite growth, we considered whether NgR(310)ecto-Fc also modulates the formation of dystrophic neurites in APPsw/PSEN-1( $\Delta$ E9) mice. In the same group of mice, clusters of dystrophic neurites were identified by anti-synaptophysin immunohistochemistry (Fig. 9*e*). Neuritic plaques are most prominent in the hippocampus, and the area occupied by synaptophysin-positive dystrophic neurite clusters is reduced in the NgR(310)ecto-Fc-treated transgenic mice (Fig. 9*f*). Microscopically, the morphology of dystrophic neurites formed in NgR(310)ecto-Fc-treated mice is similar to that in control familial AD (FAD) transgenic mice. Thus, excess NgR protein reduces both neuritic dystrophy and A $\beta$  plaque deposition in FAD transgenic mice.

### NgR causes parallel changes in sAPP $\alpha$ , sAPP $\beta$ , and A $\beta$

One mechanism by which excess NgR could reduce A $\beta$  levels is by preventing  $\alpha$ - and  $\beta$ -secretase access to APP substrate. A prediction from this model is that NgR-induced alterations in A $\beta$  will be matched by changes in sAPP levels. In contrast, if NgR were to selectively alter A $\beta$  clearance, then sAPP levels would not change when NgR levels are manipulated. If increased NgR were to favor  $\alpha$ - over  $\beta$ -secretase cleavage of APP, then sAPP $\alpha$  versus sAPP $\beta$ /A $\beta$  levels would exhibit opposite modulation by NgR.

To test these alternatives, we measured the  $\alpha$ -secretase product sAPP $\alpha$  by immunoprecipitation and immunoblot after cell culture and *in vivo* manipulations of NgR (Fig. 10). The addition of NgR(310)ecto-Fc to APPsw-N2A cultures results in a

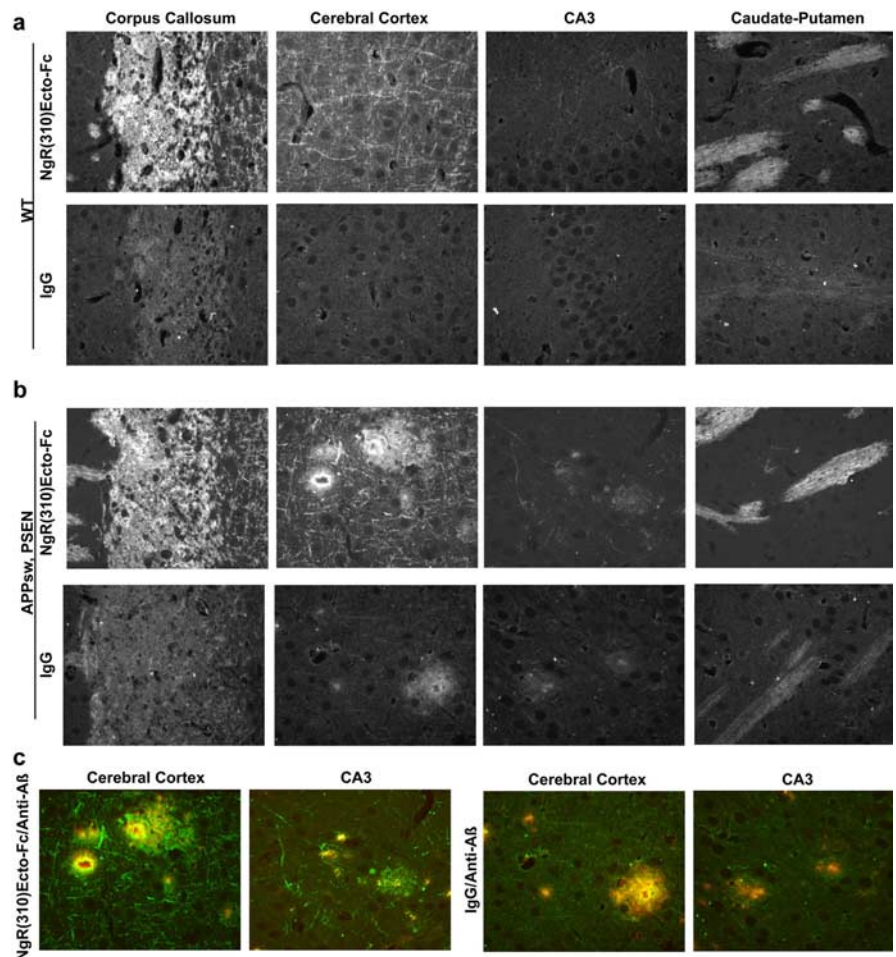


**Figure 7.** NgR(310)ecto-Fc binding sites in myelinated tracts and A $\beta$  plaque in brain sections. *a*, The binding of 0.1  $\mu$ g/ $\mu$ l NgR(310)ecto-Fc or rat IgG to adult mouse brain sections was detected by fluorescent anti-rat IgG. Note the specific staining of myelinated tracts, prominent in corpus callosum and caudate-putamen. Intracortical and hippocampal fibers are labeled to a lesser degree. Brains were fixed in paraformaldehyde, sectioned in paraffin, and treated with formic acid before staining. *b*, In brain sections from APPsw/PSEN-1 double-transgenic mice of 9 months of age, the pattern of myelinated tract staining by NgR(310)ecto-Fc but not IgG is similar to that in the wild-type (WT) animals of *a*. At this concentration, NgR(310)ecto-Fc, and to a lesser extent IgG, also binds to plaque-like structures. *c*, Double immunohistochemistry of rat NgR(310)ecto-Fc or rat IgG (green) with anti-A $\beta$  (6E10, red). Both rat NgR(310)ecto-Fc and rat IgG bind to dense A $\beta$ -positive plaque (yellow), but NgR(310)ecto-Fc is also enriched at zones of lower A $\beta$  at the edges of plaques (adjacent green).

reduction in sAPP $\alpha$  levels in the conditioned medium (Fig. 10*a,b*). *In vivo*, brains of NgR(310)ecto-Fc treated APPsw/PSEN-1( $\Delta$ E9) transgenic mice also exhibit decreased sAPP $\alpha$  levels (Fig. 10*c,d*). These reductions in sAPP $\alpha$  parallel the decreased A $\beta$  level associated with elevated NgR (Figs. 5, 9). Levels of sAPP $\alpha$  are increased in the brain of APPsw/PSEN-1( $\Delta$ E9) transgenic mice lacking NgR (Fig. 9*e,f*), matching the increase of A $\beta$  levels in these mice (Fig. 6). Levels of sAPP $\beta$  were also assessed in the transgenic mouse brain samples from knock-out mice with an antibody that selectively detects the C terminus of the transgenic sAPP $\beta$  after cleavage by  $\beta$ -secretase. Genetic ablation of NgR expression increases sAPP $\beta$ , although the magnitude of the increase is not as great as for sAPP $\alpha$  (Fig. 10*g,h*). Immunoblot detection of the C-terminal APP fragments (CTF) resulting from  $\alpha$ - or  $\beta$ -secretases reveals an increase in  $\beta$ -CTF levels;  $\alpha$ -CTF levels could not be quantitated reliably (Fig. 9*i,j*). Because NgR regulates various APP fragments and A $\beta$  levels in parallel, we conclude that NgR/APP association reduces cleavage of APP by both  $\alpha$ - and  $\beta$ -secretases.

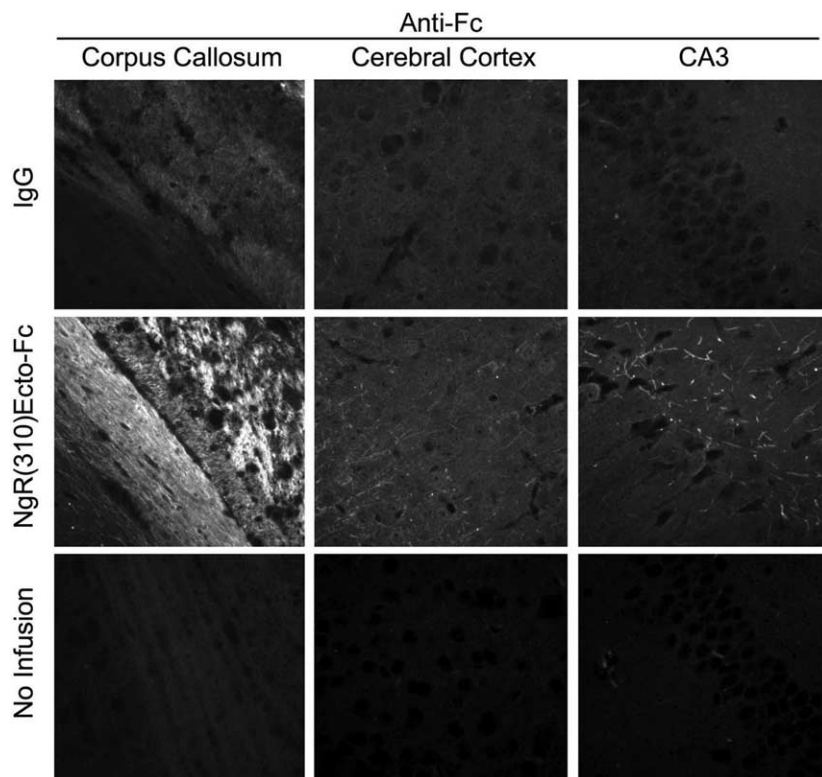


**Figure 8.** Localization of NgR(310)ecto-Fc after intracerebroventricular infusion. Brain sections were prepared from APPsw/PSEN-1 double-transgenic mice of 7 months of age after infusion with rat IgG, rat NgR(310)ecto-Fc, or no protein. The distribution of the infused protein was detected with fluorescently tagged anti-rat Fc and is similar to that of *in vitro* protein binding in Figure 6.

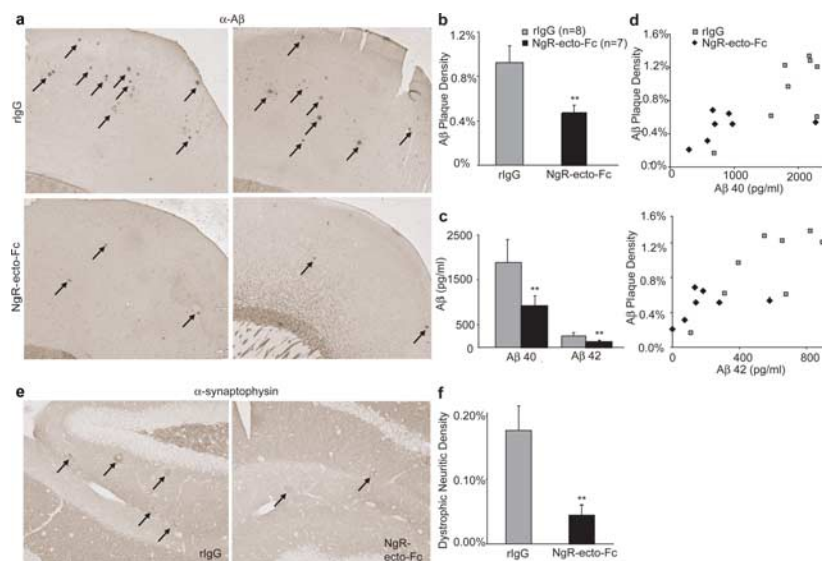


**Figure 9.** NgR-ecto-Fc decreases A $\beta$  plaque formation and dystrophic neurites *in vivo*. Transgenic mice expressing both the human APPsw and PSEN-1( $\Delta$ E9) protein were treated from 6–8 months of age with either rat IgG or rat NgR(310)ecto-Fc from a minipump connected to an intracerebroventricular catheter. Each mouse received 0.4 mg of protein over 2 months ( $0.29 \text{ mg} \cdot \text{kg}^{-1} \cdot \text{d}^{-1}$ ). **a, b**, Transgenic mice were processed for A $\beta$  immunohistochemistry to reveal amyloid plaque deposition at 8 months of age (**a**). The arrows indicate examples of plaque deposits in sections of the cerebral cortex from three representative mice of eight or seven mice in each group. The area of cerebral cortex occupied by plaque was quantitated (**b**). Data are means  $\pm$  SEM from  $n = 8$  or 7 mice. The decrease in A $\beta$ -positive plaques in the NgR(310)ecto-Fc group compared with control is significant ( $**p \leq 0.02$ , Student's *t* test). **c**, A $\beta$  was measured in formic acid extracts of brain. Data are means  $\pm$  SEM from nine animals in each group. The decrease in A $\beta$  in the NgR(310)ecto-Fc group compared with IgG is significant ( $**p \leq 0.02$ , Student's *t* test). The ratio of A $\beta_{40}$  to A $\beta_{42}$  is not altered in the NgR(310)ecto-Fc-treated group. **d**, Correlation of plaque density and A $\beta_{40}$  or A $\beta_{42}$  levels in mice treated as in **a–c**. **e, f**, Anti-synaptophysin-immunoreactive dystrophic neurites in control and NgR(310)ecto-Fc-treated transgenic hippocampus are illustrated (arrows, **e**). The percentage of area occupied by synaptophysin-positive dystrophic neurites is reported in **f**. Data are means  $\pm$  SEM from eight or seven mice per group.  $**p < 0.02$ , Student's *t* test; the decrease in dystrophic neurites with NgR(310)ecto-Fc treatment is significant.

## Discussion

Several lines of evidence presented here indicate that the NgR protein plays a significant role in APP/A $\beta$  pathophysiology. Neuronal NgR localization is altered in AD brain. NgR protein physically associates with APP. Endogenous NgR/APP/A $\beta$  interaction serves to suppress the production of A $\beta$  and the A $\beta$  plaque deposition that is characteristic of AD. Alterations of NgR function by gene targeting or by infusion of soluble NgR(310)ecto-Fc regulate A $\beta$  levels in transgenic mouse brain. There is an inverse relationship between the level of NgR and the level of A $\beta$ , plaque deposits, and neuritic dystrophy. Elimination of NgR expression increases these measures of AD activity, whereas treatment with excess soluble NgR protein reduces A $\beta$ , plaques, and neuritic dystrophy.

The metabolism of APP and A $\beta$  consists of numerous steps that must be considered in explaining the effects of NgR on A $\beta$ . Certain steps are unlikely to play a significant role based on the current studies. Because A $\beta$  levels, amyloid plaque deposition, and neuritic dystrophy change in parallel, it is unlikely that A $\beta$  aggregation or the induction of dystrophy is strongly altered by NgR. The extracellular location of NgR and the absence of any alteration in A $\beta_{40}$ /A $\beta_{42}$  ratio with NgR manipulations argue that  $\gamma$ -secretase is not a major site of NgR modulation of APP/A $\beta$  pathology. Exogenous soluble NgR(310)ecto-Fc appears to enhance endogenous NgR action, acting in opposition to NgR gene deletion. Therefore, NgR-mediated signaling for axon outgrowth inhibition is unlikely to play a central role for the ability of NgR to reduce A $\beta$  pathology. If, instead, NgR signaling within neurons were crucial, then the soluble decoy receptor would have identical (not opposite) effects to those of NgR gene disruption. It is also unlikely that the effects of extracellular NgR(310)ecto-Fc on A $\beta$  pathology can be explained primarily by altered intracellular APP trafficking. Could the formation of an A $\beta$  complex with cell surface endogenous NgR or extracellular NgR(310)ecto-Fc alter the degradation or clearance of the peptide? Specifically, might exogenous NgR(310)ecto-Fc lower A $\beta$  by acting as a “sink” to remove A $\beta$  in the same manner as does anti-A $\beta$  antibody? The limiting effect of endogenous NgR on A $\beta$  pathology and the ability of NgR overexpression in neuroblastoma cells to reduce A $\beta$  suggest that a sink hypothesis does not explain the principal action of NgR on A $\beta$  pathology.



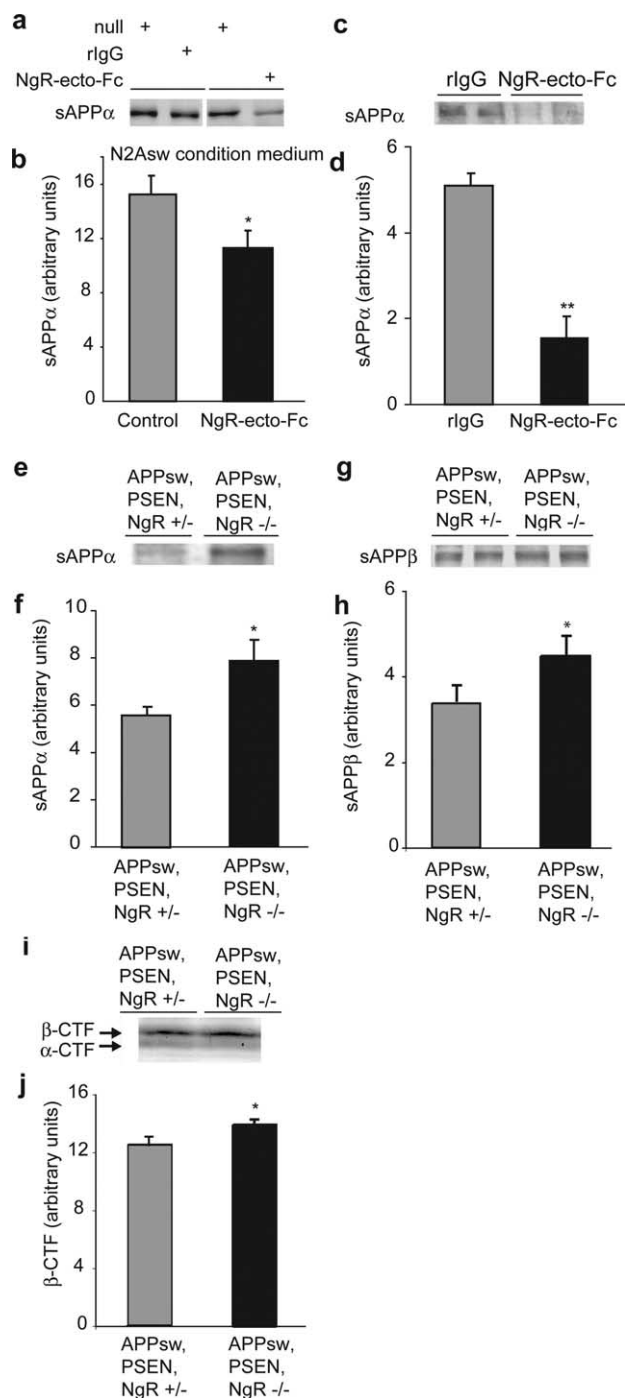


**Figure 10.** NgR regulates sAPP $\alpha$  in parallel with A $\beta$  levels. The level of sAPP $\alpha$  in brain extracts or N2A culture medium was analyzed by immunoprecipitation with anti-N-terminal-APP 22C11 antibody and immunoblot with anti-A $\beta$ <sub>1–17</sub> 6E10 antibody. The sAPP $\beta$  fragment was analyzed in brain tissue by direct immunoblots with anti-sAPP $\beta$ sw C-terminal antibody, and the CTFs were detected by the anti-APP-C-terminal 369 antibody. Immunoreactivity per milligram of protein was assessed in independent samples for  $n = 6–9$  mice or cell cultures in each experimental group (mean  $\pm$  SEM; \* $p < 0.05$  level, \*\* $p < 0.01$ , Student's  $t$  test). **a, b**, sAPP $\alpha$  levels in conditioned medium from APPsw-expressing N2A cells was quantitated after 48 h culture in the presence of 1 mg/ml control rat IgG or rat NgR(310)ecto-Fc. **c, d**, sAPP $\alpha$  in brain extracts from APPsw/PSEN-1( $\Delta$ E9) transgenic mice treated from 6–8 months of age with either rat IgG or rat NgR(310)ecto-Fc intracerebroventricularly, as in Figure 9. **e, f**, sAPP $\alpha$  in brain extracts from 6-month-old littermate-matched mice transgenic for APPsw/PSEN-1( $\Delta$ E9) and either NgR $^{+/-}$  or NgR $^{-/-}$ , as in Figure 6. **g, h**, sAPP $\beta$  in brain extracts from 13-month-old littermate-matched mice transgenic for APPsw/PSEN-1( $\Delta$ E9) and either NgR $^{+/-}$  or NgR $^{-/-}$ . **i, j**,  $\alpha$ -CTF and  $\beta$ -CTF in brain extracts from 13-month-old littermate-matched mice transgenic for APPsw/PSEN-1( $\Delta$ E9) and either NgR $^{+/-}$  or NgR $^{-/-}$ . The  $\beta$ -CTF level is quantitated in **j**.

These considerations imply that NgR blockade of initial  $\alpha$ -secretase and  $\beta$ -secretase cleavage of APP is likely to be a principal site of NgR action *in vivo*. Because NgR binds to the extracellular region of APP that serves as a secretase substrate, NgR might serve as a competitive inhibitor of processing. Alternatively, the APP/NgR interaction may indirectly reduce APP access to secretase compartments in the cell. Consistent with NgR-mediated blockade of both  $\alpha$ - and  $\beta$ -secretase access to APP, we found that the levels of the sAPP $\alpha$ , sAPP $\beta$ , and  $\beta$ -CTF fragment are altered in parallel with A $\beta$  levels in NgR $^{-/-}$  mice and NgR(310)ecto-Fc-treated mice. Together, the data are consistent with the hypothesis that NgR reduces A $\beta$  pathology primarily by reducing  $\alpha$ - and  $\beta$ -secretase cleavage.

Apart from A $\beta$  pathophysiology and AD, NgR interactions with APP and A $\beta$  may play roles in normal neuronal physiology. Because APP has been identified as an adaptor for kinesin-dependent transport of certain cargos in the axon (Kamal et al., 2001), NgR localization to the distal axon may depend on binding to APP. Studies of NgR distribution and function in APP null mice should resolve this issue. Although we did not observe direct competition between A $\beta$  and Nogo-66, myelin-associated glycoprotein (MAG), or oligodendrocyte myelin glycoprotein for NgR binding (data not shown), there may be modulatory effects of APP or A $\beta$  on axon growth inhibition by CNS myelin under certain conditions distinct from those examined in preliminary experiments. Because A $\beta$  has been implicated as a regulator of synaptic function recently (Walsh et al., 2002b; Kamenetz et al., 2003), NgR may participate in this modulation directly or indirectly. Overall, the association of APP and NgR tightens the links between axonal function and the neurodegenerative process in AD.

## References

- Borchelt DR, Ratovitski T, van Lare J, Lee MK, Gonzales V, Jenkins NA, Copeland NG, Price DL, Sisodia SS (1997) Accelerated amyloid deposition in the brains of transgenic mice coexpressing mutant presenilin 1 and amyloid precursor proteins. *Neuron* 19:939–945.
- Chen MS, Huber AB, van der Haar ME, Frank M, Schnell L, Spillmann AA, Christ F, Schwab ME (2000) Nogo-A is a myelin-associated neurite outgrowth inhibitor and an antigen for monoclonal antibody IN-1. *Nature* 403:434–439.
- Dineley KT, Westerman M, Bui D, Bell K, Ashe KH, Sweatt JD (2001)  $\beta$ -Amyloid activates the mitogen-activated protein kinase cascade via hippocampal  $\alpha 7$  nicotinic acetylcholine receptors: *in vitro* and *in vivo* mechanisms related to Alzheimer's disease. *J Neurosci* 21:4125–4133.
- Ehehalt R, Keller P, Haass C, Thiele C, Simons K (2003) Amyloidogenic processing of the Alzheimer beta-amyloid precursor protein depends on lipid rafts. *J Cell Biol* 160:113–123.
- Fournier AE, GrandPre T, Strittmatter SM (2001) Identification of a receptor mediating Nogo-66 inhibition of axonal regeneration. *Nature* 409:341–346.
- Fournier AE, Gould GC, Liu BP, Strittmatter SM (2002) Truncated soluble Nogo receptor binds Nogo-66 and blocks inhibition of axon growth by myelin. *J Neurosci* 22:8876–8883.
- Gentleman SM, Nash MJ, Sweeting CJ, Graham DI, Roberts GW (1993) Beta-amyloid precursor protein (beta APP) as a marker for axonal injury after head injury. *Neurosci Lett* 160:139–144.
- GrandPre T, Nakamura F, Vartanian T, Strittmatter SM (2000) Identification of the Nogo inhibitor of axon regeneration as a Reticulon protein. *Nature* 403:439–444.
- GrandPre T, Li S, Strittmatter SM (2002) Nogo-66 receptor antagonist peptide promotes axonal regeneration. *Nature* 417:547–551.
- Hardy J, Selkoe DJ (2002) The amyloid hypothesis of Alzheimer's disease: progress and problems on the road to therapeutics. *Science* 297:353–356.
- He W, Lu Y, Qahwash I, Hu XY, Chang A, Yan R (2004) Reticulon family members modulate BACE1 activity and amyloid-beta peptide generation. *Nat Med* 10:959–965.
- Jankowsky JL, Xu G, Fromholt D, Gonzales V, Borchelt DR (2003) Environ-

- mental enrichment exacerbates amyloid plaque formation in a transgenic mouse model of Alzheimer disease. *J Neuropathol Exp Neurol* 62:1220–1227.
- Kamal A, Almenar-Queralt A, LeBlanc JF, Roberts EA, Goldstein LS (2001) Kinesin-mediated axonal transport of a membrane compartment containing beta-secretase and presenilin-1 requires APP. *Nature* 414:643–648.
- Kamenetz F, Tomita T, Hsieh H, Seabrook G, Borchelt D, Iwatsubo T, Sisodia S, Malinow R (2003) APP processing and synaptic function. *Neuron* 37:925–937.
- Kim JE, Li S, GrandPre T, Qiu D, Strittmatter SM (2003) Axon regeneration in young adult mice lacking Nogo-A/B. *Neuron* 38:187–199.
- Kim JE, Liu BP, Park JH, Strittmatter SM (2004) Nogo-66 receptor prevents raphespinal and rubrospinal axon regeneration and limits functional recovery from spinal cord injury. *Neuron* 44:439–451.
- Klein WL (2002) Abeta toxicity in Alzheimer's disease: globular oligomers (ADDLs) as new vaccine and drug targets. *Neurochem Int* 41:345–352.
- Kuner P, Schubel R, Hertel C (1998) Beta-amyloid binds to p57NTR and activates NFkappaB in human neuroblastoma cells. *J Neurosci Res* 54:798–804.
- Lazarov O, Lee M, Peterson DA, Sisodia SS (2002) Evidence that synaptically released  $\beta$ -amyloid accumulates as extracellular deposits in the hippocampus of transgenic mice. *J Neurosci* 22:9785–9793.
- Lee JK, Kim JE, Sivula M, Strittmatter SM (2004) Nogo receptor antagonism promotes stroke recovery by enhancing axonal plasticity. *J Neurosci* 24:6209–6217.
- Li S, Strittmatter SM (2003) Delayed systemic Nogo-66 receptor antagonist promotes recovery from spinal cord injury. *J Neurosci* 23:4219–4227.
- Li S, Liu BP, Budel S, Li M, Ji B, Walus L, Li W, Jirik A, Rabacchi S, Choi E, Worley D, Sah DW, Pepinsky B, Lee D, Relton J, Strittmatter SM (2004) Blockade of nogo-66, myelin-associated glycoprotein, and oligodendrocyte myelin glycoprotein by soluble nogo-66 receptor promotes axonal sprouting and recovery after spinal injury. *J Neurosci* 24:10511–10520.
- Lombardo JA, Stern EA, McLellan ME, Kajdasz ST, Hickey GA, Bacskai BJ, Hyman BT (2003) Amyloid- $\beta$  antibody treatment leads to rapid normalization of plaque-induced neuritic alterations. *J Neurosci* 23:10879–10883.
- McGee AW, Strittmatter SM (2003) The Nogo-66 receptor: focusing myelin inhibition of axon regeneration. *Trends Neurosci* 26:193–198.
- Nagele RG, D'Andrea MR, Anderson WJ, Wang HY (2002) Intracellular accumulation of beta-amyloid(1–42) in neurons is facilitated by the alpha 7 nicotinic acetylcholine receptor in Alzheimer's disease. *Neuroscience* 110:199–211.
- Otsuka N, Tomonaga M, Ikeda K (1991) Rapid appearance of beta-amyloid precursor protein immunoreactivity in damaged axons and reactive glial cells in rat brain following needle stab injury. *Brain Res* 568:335–338.
- Prinjha R, Moore SE, Vinson M, Blake S, Morrow R, Christie G, Michalovich D, Simmons DL, Walsh FS (2000) Inhibitor of neurite outgrowth in humans. *Nature* 403:383–384.
- Scott JN, Parhad IM, Clark AW (1991) Beta-amyloid precursor protein gene is differentially expressed in axotomized sensory and motor systems. *Brain Res Mol Brain Res* 10:315–325.
- Selkoe DJ, Schenk D (2003) Alzheimer's disease: molecular understanding predicts amyloid-based therapeutics. *Annu Rev Pharmacol Toxicol* 43:545–584.
- Sheng JG, Price DL, Koliatsos VE (2002) Disruption of corticocortical connections ameliorates amyloid burden in terminal fields in a transgenic model of A $\beta$  amyloidosis. *J Neurosci* 22:9794–9799.
- Thinakaran G, Teplow DB, Siman R, Greenberg B, Sisodia SS (1996) Metabolism of the "Swedish" amyloid precursor protein variant in neuro2a (N2a) cells. Evidence that cleavage at the "beta-secretase" site occurs in the golgi apparatus. *J Biol Chem* 271:9390–9397.
- Walsh DM, Klyubin I, Fadeeva JV, Rowan MJ, Selkoe DJ (2002a) Amyloid-beta oligomers: their production, toxicity and therapeutic inhibition. *Biochem Soc Trans* 30:552–557.
- Walsh DM, Klyubin I, Fadeeva JV, Cullen WK, Anwyl R, Wolfe MS, Rowan MJ, Selkoe DJ (2002b) Naturally secreted oligomers of amyloid beta protein potentially inhibit hippocampal long-term potentiation in vivo. *Nature* 416:535–539.
- Wang HY, Lee DH, D'Andrea MR, Peterson PA, Shank RP, Reitz AB (2000) beta-Amyloid(1–42) binds to alpha7 nicotinic acetylcholine receptor with high affinity. Implications for Alzheimer's disease pathology. *J Biol Chem* 275:5626–5632.
- Wang X, Chun SJ, Treloar H, Vartanian T, Greer CA, Strittmatter SM (2002) Localization of Nogo-A and Nogo-66 receptor proteins at sites of axon-myelin and synaptic contact. *J Neurosci* 22:5505–5515.
- Yang X, Hyder F, Shulman RG (1996) Activation of single whisker barrel in rat brain localized by functional magnetic resonance imaging. *Proc Natl Acad Sci USA* 93:475–478.